Prediction of the Conversion Efficiency of a GaSb Thermophotovoltaic Converter Heated by Radioisotope Source

F. Bouzid*‡

*Laboratory of Metallic and Semiconducting Materials, University of Biskra, P.B.145, Biskra, 07000, Algeria.

faycal.bouzid@ymail.com

‡Corresponding Author; F. Bouzid, LMSM, University of Biskra, P.B.145, Biskra, 07000, Algeria, Tel: +213 (0)33741087, Fax: +213 (0)33741087, faycal.bouzid@ymail.com

Received: 08.08.2013 Accepted: 13.09.2013

Abstract- In recent years, Gallium Antimonide (GaSb), which has smallest bandgap among III-V semiconductors family, became the subject of extensive investigations in the field of thermophotovoltaic (TPV) converters, because of the recent improvements in optoelectronic technology. In this paper, we investigated the heat to electricity conversion efficiency of a GaSb radioisotope thermophotovoltaic (RTPV) converter, taking account of the photons with energy below the cells bandgap using a comprehensive analytical process. The results show that a conversion efficiency greater than 28% can be obtained for radiator's temperature of 1600k, at ambiant temperature. This efficiency will decrease as the cell temperature increase.

Keywords- Radioisotope; Emissivity; Thermophotovoltaic; Efficiency; Temperature.

1. Introduction

Thermophotovoltaic converters are devices in which a photovoltaic (PV) device converts the infrared radiation emitted by heated body, often called radiator, into electric power [1]. The radiator, generally made by refractory materials such as Tungsten [2] or ceramic oxides [3], may be heated by the ignition of a fuel, highly concentrated sunlight or by using radio-isotopic power sources [4] as described in figure 1.

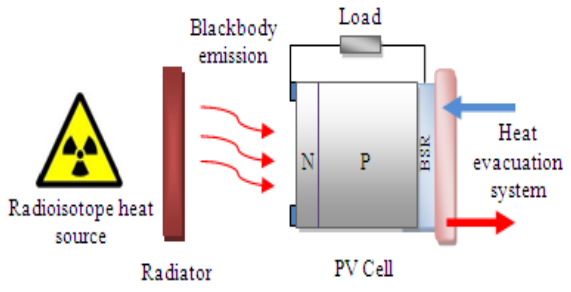

Fig. 1. Principle of thermophotovoltaic conversion.

A TPV system powered by radioisotope decay, as an alternative source of power, is a potential power system used in current deep space satellites, where the solar radiation energy density is too low for a conventional PV power system to be used [5].

In order to make the process efficient, the energy of the photons reaching the PV cell must be superior to the bandgap energy of the cell. For this reason, GaSb and its related ternary and quaternary alloys have been considered as promising materials for TPV applications because of their low bandgap energies. These cells are able to convert a larger part of the infrared spectrum, and therefore have the potential to give high efficiency and power output at moderate radiator temperature.

To increase the efficiency which is determined by energy absorbed relative to total incoming radiation, the remainder of the spectrum must be reflected back to the radiator. Thereby a back surface reflector (BSR) is often employed in the design of conventional TPV cells. This creates the concept of "photon recycling" whereby photons with energies less than optimum for conversion are sent back to the radiator for recycling until they come back at the proper energy [6].

For efficient RTPV conversion, the radioisotope source need a number of important requirements such as: high temperature of the heat source, decays without too much gamma or neutron emission, a long half-life of several years or decades so that extended missions are supported and high

decay energy per isotope mass. Some current RTPV systems use ^{238}Pu isotope as a heat source since, in a pure form, ^{238}Pu can reach surface temperature of 1300k [7], others uses $^{238}PuO_2$ with molybdenum multi-foil insulations which can withstand hot side temperature up to 1500k [5,8]. However, recently published works show that the ^{90}Sr isotope meets all the above mentioned requirements [9]. The current TPV cell technology is approaching 30% cell efficiency at 300k due steady improvement in MOCVD manufacturing process. Through the use of dual junction cells to convert below bandgap photons, further improvements in the cell efficiency are expected to take place over the next few years with expectations of approaching 40% [10].

In this work, the theoretical efficiency of GaSb RTPV cells is computed using a comprehensive model in which the cells are exposed to radiation from a blackbody radiator in the 1300k to 1600k temperature range. The influences of the base region doping profile, the cell thickness, the radiator emissivity and the cell temperature on the conversion efficiency have been investigated in order to find an optimum energy conversion system.

2. Model description

Figure 2 show a simplified structure of a GaSb TPV cell, where x_j is the junction depth, w is the depletion region width, H is the P-type quasi neutral region and d is the cell thickness.

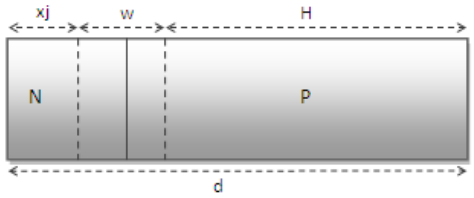

Fig. 2. Simplified configuration of a GaSb TPV cell.

In our calculations, the effect of the back surface field (BSF) is not taken into account for the sake of simplicity, no structural losses and contact shadowing for the cells and the values of the physical and geometrical parameters were chosen from various published papers.

2.1. Analytical model

The determination of the TPV cell efficiency implies knowledge of its current voltage characteristic under illumination which can be written as [11]:

$$I_{Total} = I_{Ph} - I_D \tag{1}$$

Where I_D is the dark current (in the absence of irradiation), and I_{ph} is the current excited by the incident radiations, i. e., the photocurrent for the so-called ideal model.

The dark current is described by the Shockley diode equation:

$$I_D = I_0 \cdot \left[\exp\left(\frac{qv}{kT}\right) - 1 \right] \tag{2}$$

Where q is the elementary charge, K is the Boltzmann constant, T is the temperature and I_0 is the reverse saturation current, given by equation (3) [11], using the cell design shown in figure 2:

$$I_0 = \frac{qSD_e n_i^2}{l_e N_a} \cdot \frac{\frac{s_e l_e}{D_e}\cosh(\frac{H}{l_e}) + \sinh(\frac{H}{l_e})}{\frac{s_e l_e}{D_e}\sinh(\frac{H}{l_e}) + \cosh(\frac{H}{l_e})} + \frac{qSD_h n_i^2}{l_h N_d} \cdot \frac{\frac{s_h l_h}{D_h}\cosh(\frac{x_j}{l_h}) + \sinh(\frac{x_j}{l_h})}{\frac{s_h l_p}{D_h}\sinh(\frac{x_j}{l_h}) + \cosh(\frac{x_j}{l_h})} \tag{3}$$

Where n_i is the intrinsic carrier concentration calculated from the relation:

$$n_i^2 = N_c N_v \exp(-\frac{Eg}{kT}) \tag{4}$$

Where N_c and N_v are the effective densities of states in the conduction and valence bands respectively; Eg is the bandgap energy; N_a and N_d are the acceptor and donor concentrations; S_h and S_e are the recombination velocities in the N and P-type regions; S is the cell surface; D_e and D_h are the diffusion constants of electrons and holes respectively, calculated from Einstein relationship:

$$D_{e/h} = \frac{kT}{q}\mu_{e/h} \tag{5}$$

Where μ_e and μ_h are mobilities of the electrons and holes respectively; l_e and l_h are the minority carrier diffusion lengths of electrons and holes respectively, calculated according to the following formula [11]:

$$l_{e/h} = \sqrt{D_{e/h} \cdot \tau_{e/h}} \tag{6}$$

Where τ_e and τ_h are the minority carrier lifetimes of the electrons and holes respectively. The minority carrier lifetime is defined as the average time it takes an excess minority carrier to recombine. It is extremely sensitive to smallest amounts of impurities or intrinsic defects [11]:

$$\tau_{e/h} = \frac{1}{N_{T,D/A} \cdot \sigma_{e/h} \cdot V_{t_{e/h}}} \tag{7}$$

Where N_{TD} and N_{TA} are the concentrations of donor and acceptor traps; Vt_e and Vt_h are the thermal velocities for electrons and holes; σ_e and σ_h are the capture cross sections for electrons and holes respectively.

The photocurrent I_{ph} is given by the sum of the photocurrents generated in the emitter, the base and the depleted region of the cell.

$$I_{Ph} = \int_0^{\lambda max} q \cdot S \cdot F(\lambda) \cdot SR(\lambda) d\lambda \quad (8)$$

Where λ is the wavelength of the incident photon, λ_{max} is the cutoff wavelength corresponding to the bandgap energy; its expression is given as:

$$\lambda_{max} = \frac{h \cdot c}{E_g} \quad (9)$$

Where h is the Planck's constant and c is the speed of light.

SR(λ) is the internal spectral response of the TPV cell given by the sum of the contribution from the emitter, the base and the depleted region as described in equation (10):

$$SR(\lambda) = SR_E(\lambda) + SR_B(\lambda) + SR_{DR}(\lambda) \quad (10)$$

F(λ) is the spectral photons flux of the incident radiation that was absorbed by the TPV cell. Its expression for $\lambda < \lambda_{max}$ could be written as [12,13]:

$$F(\lambda) = \chi \cdot \frac{2\pi \cdot c}{\lambda^4 \left(e^{\frac{hc}{\lambda k T_{Rad}}} - 1 \right)} \quad (11)$$

Where T_{Rad} is the TPV radiator temperature and χ is the effective cavity emissivity that characterizes the performance of the spectral control in TPV system.

The value of χ is taken as 0.78 based on the best reported spectral control system performance.

2.2. Photovoltaic parameters

The open circuit voltage is expressed as [11]:

$$V_{oc} = \frac{nkT_{Cell}}{q} \cdot \ln\left(\frac{I_{sc}}{I_0} + 1 \right) \quad (12)$$

Where n is the factor of ideality assumed to be 1 for GaSb TPV cells based on ref. [14], I_{sc} is the short circuit current, and T_{Cell} is the cell temperature.

The power delivered by the cell is given by the product of the cell voltage and current, and was maximized by satisfying the condition:

$$\frac{d(I_{Total} \cdot V)}{dI} = 0 \quad (13)$$

The fill factor is defined by:

$$FF = \frac{I_m \cdot V_m}{I_{sc} \cdot V_{oc}} \quad (14)$$

Where I_m and V_m are coordinates of the maximum power point (P_{max}).

The overall conversion efficiency of a TPV system, supposing that no resistive losses, can be expressed as [15]:

$$\eta = \frac{I_{sc} \cdot V_{oc} \cdot FF}{P_{Inc} - P_{Ret}} \quad (15)$$

Where P_{Inc} is the total incident radiation power integrated over all frequencies and P_{Ret} is the power returned to the radiator, since photons not absorbed are able to be recycled.

The sequence of calculations to obtain the current-voltage characteristics and the conversion efficiency at a given radiator temperature is sketched in the flowchart in figure 3 below:

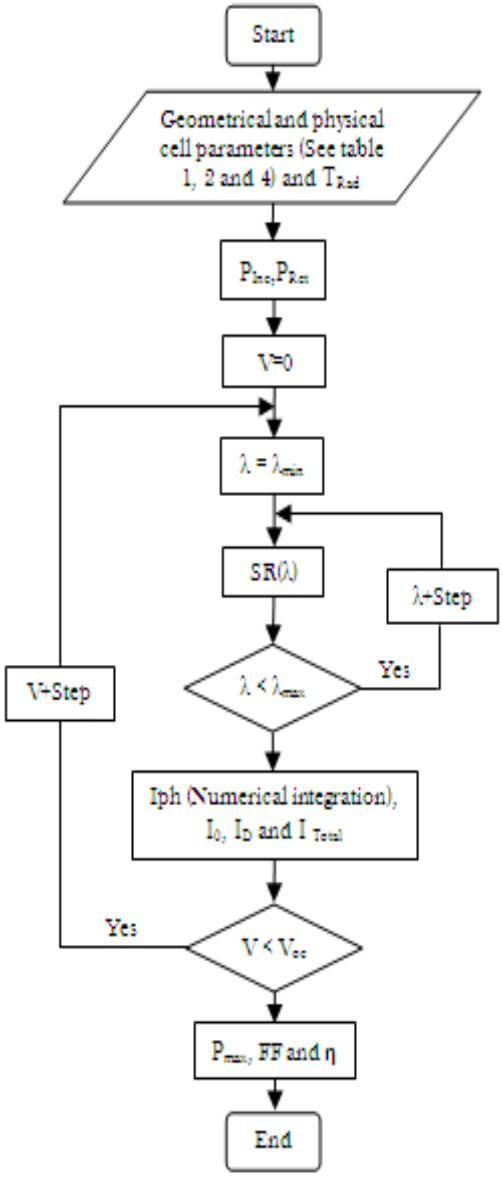

Fig. 3. Analytical model flowchart.

2.3. GaSb parameter equations

L.G. Ferguson et al. [14] suggested a semi empirical equation for the temperature dependence of the bandgap energy of the form:

$$Eg = 0.813 - \frac{(6\times10^{-4})\cdot T^2}{(T+265)} \quad (16)$$

This equation was based on the observation that the energy gap should be proportional to T at high temperatures and proportional to T^2 at low temperatures.

The Mobility of both electrons and holes is calculated as a function of doping and temperatures using the Caughey – Thomas empirical model [16,17,18] given as:

$$\mu_{e/h}(N_{a/d}, T_{Cell}) = \mu_{min,e/h} + \frac{\mu_{max,e/h}\cdot(300/T_{Cell})^{\theta_{1},e/h} - \mu_{min,e/h}}{1+[N_{a/d}/N_{ref,e/h}(T_{Cell}/300)^{\theta_{2},e/h}]^{\alpha_{e/h}}} \quad (17)$$

Where $\mu_{min,e/h}$ and $\mu_{max,e/h}$ represents the value that mobility reaches for very low and high doping level, $N_{ref,e/h}$ is the doping concentration at which the mobility is decreased to half the value is reaches at low doping at room temperature. $\theta_{1,e/h}$, $\theta_{2,e/h}$ and $\alpha_{e/h}$ are respectively the suggested fitting parameters [16].

All the value of parameters used for the simulation of the carrier's mobility has been summarized in **Table 1**.

Table 1. Parameters used in the simulation of GaSb carrier mobilities.

$\mu_{min,e}$ [cm²/vs]	$\mu_{max,e}$ [cm²/vs]	$\mu_{min,h}$ [cm²/vs]	α_e	$\theta_{1,e}$	$\theta_{1,h}$
1050	5650	190	1.05	2	1.7
$\mu_{max,h}$ [cm²/vs]	$N_{ref,e}$ [cm^{-3}]	$N_{ref,h}$ [cm^{-3}]	α_h	$\theta_{2,e}$	$\theta_{2,h}$
875	$2.8e^{17}$	$9e^{17}$	0.65	2.8	2.7

The absorption coefficient of GaSb was calculated using the direct bandgap semi-conductor expression given as [19]:

$$\alpha(E) = K_{abs}\sqrt{(E-Eg)} \quad (18)$$

$$K_{abs} = \frac{q^2\chi_{vc}^2(2m_r)^{3/2}}{\lambda_{max}\varepsilon_0\hbar^3 n_{op}} \quad (19)$$

$$\chi_{vc} = \frac{\hbar}{Eg}\sqrt{\frac{Ep}{3m_0}} \quad (20)$$

Where E is the incoming photon energy, E_p is the Kane's energy, m_0 is the electron rest mass, n_{op} is the optical refraction index and m_r is the reduced effective mass.

The specific parameters χ_{vc}, m_r, λ_{max} and n_{op} used in the simulation are given in **Table 2**.

Table 2. Specific parameters used to calculate the absorption coefficient of GaSb.

χ_{vc} [A°]	m_r	λ_{max} [m]	n_{op} [20]	ξ_0 [F/m]
2.63	0.043	$1.72e^{-6}$	3.8	$8.85e^{-12}$

The relative dielectric constant of GaSb is taken to be 15.7 [19].

The effective masses for electrons and holes are given by the expressions:

$$m_e^* = 0.047 \times m_0 \quad [19] \quad (21)$$

$$m_h^* = 0.50 \times m_0 \quad [21] \quad (22)$$

The effective densities of states N_c and N_v are given as [22]:

$$Nc = 4\times10^{13}\times T^{1.5} \quad (23)$$

$$Nv = 3.5\times10^{15}\times T^{1.5} \quad (24)$$

2.4. Incident light spectrum

Figure 4 gives a general idea of how much light is accessible to a PV cell made of GaSb. The colored portions in the figure indicate the fraction of the photon spectrum that is above the bandgap energy.

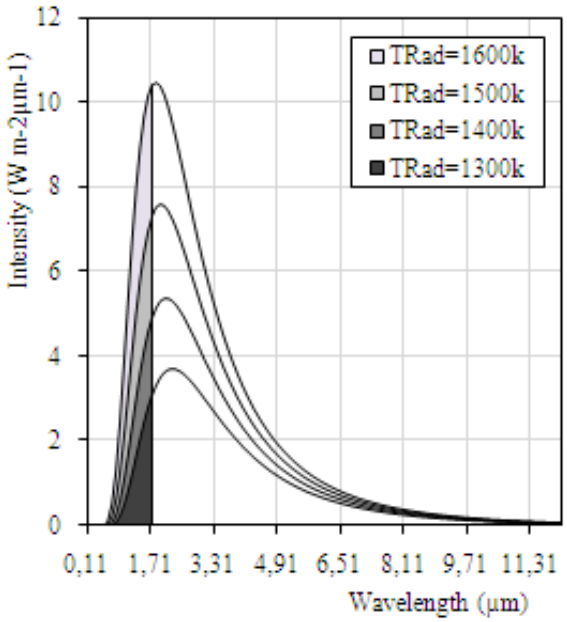

Fig. 4. Blackbody spectral irradiance for $\chi = 0.78$.

Table 3 below indicates the fraction of incident light with energies below the cell's bandgap calculated by integrating the spectral irradiance under the blackbody curve for $\lambda > \lambda_{max}$, and the total incident radiation power P_{Inc}.

Table 3. Percentage of incident radiations with energies below the GaSb bandgap for $\chi = 0.78$, and the total incident radiation power P_{Inc}.

T_{Rad} (k)	1300	1400	1500	1600
Returned power (%)	87.44	83.83	80.04	76.16
P_{Inc}(w/m²)	12.53	16.87	22.26	28.84

3. Results and discussion

3.1. Effect of the base region profile and cell thickness

The level of doping plays a crucial role in the performance of TPV devices. To reveal the potential effect brought by the base region doping profile, we have simulated and plotted the conversion efficiency versus different doping levels in figure 5.

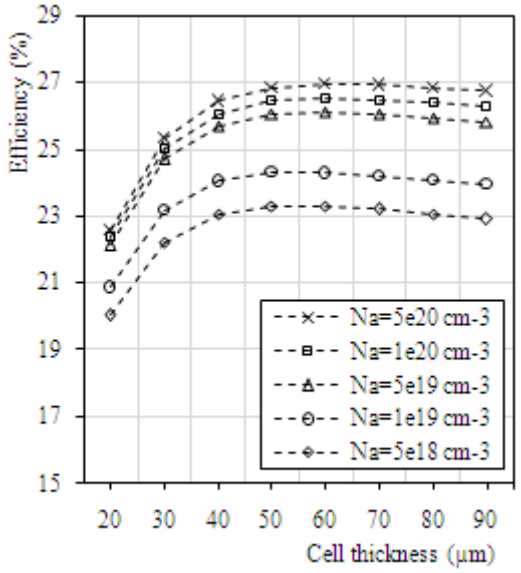

Fig. 5. Effect of the base region profile and cell thickness on the conversion efficiency.

The analysis starts by assuming the values assigned for the cell parameters, presented in **Table 4**.

Table 4. Cell parameters used in simulations for T_{Cell} = 300k and T_{Rad} = 1500k.

χ	Nd [cm^{-3}]	Eg [eV]
0.78	$5e^{19}$	0.72
N_{TD} [cm^{-3}]	N_{TA} [cm^{-3}]	Vt_e [cm/s][22]
$1.2e^{17}$	$7.56e^{13}$	$5.8e^{7}$
S_e [cm/s]	S_h [cm/s]	x_j [µm]
1000	5000	0.4

Vt_h [cm/s][22]	σ_e [cm²][23]	σ_h [cm²][23]
$2.1e^{7}$	$8e^{-19}$	$9e^{-15}$

It can be seen from Figure 5 above that the maximum value of the base region doping concentration is about $5e^{20}$ cm^{-3}. At the same time, it is clear that the efficiency increases significantly with increasing the cell thickness. Where, In case of Na = $5e^{20}$ cm^{-3}, the efficiency curve shows an improvement from 22.59% to 26.96% for 20µm and 60µm cell's thickness respectively for the reason that, in case of thin thickness, most of the incident photons are not absorbed resulting in a lower efficiency. However, when the cell thickness exceeds 60µm, we note a weak reduction in the conversion efficiency due to the recombination phenomenon, since the free carriers generated deeper in the bulk have to travel longer before being collected. So a cell thickness of about 60µm is needed to lose not too much of the efficiency

3.2. Effect of the front recombination velocity

In this work, the back surface recombination velocity was fixed at 1000 cm/s, and the influence of the front recombination velocity on the conversion efficiency has been simulated, where values of 5000, 10000 and 50000 cm/s was used for different cell thicknesses with T_{Rad} = 1500k, T_{Cell} = 300k, $N_a = 5e^{20}cm^{-3}$and χ = 0.78 .

From figure 6 below, it is apparent that the efficiency drops notably with increasing the front recombination velocity, since most of the photo-generated carriers cannot be collected by the electrodes what implies a low electric current. The maximum conversion efficiency obtained for 60µm cell thickness can attain 26.96% for a front recombination velocity equals to 5000cm/s. Therefore, to reduce the power loss, the front surface recombination velocity should not exceed 5000cm/s.

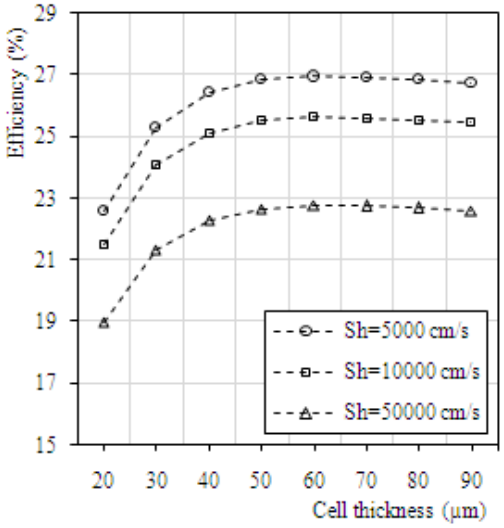

Fig. 6. Effect of the front surface recombination velocity and cell thickness on the conversion efficiency.

3.3. Effect of the radiator effective cavity emissivity

The radiator exhibits a high emissivity in the spectral range usable for the PV cell, and a low emissivity elsewhere. The emissivity of Tungsten and ceramic oxides based on Erbium and Ytterbium, frequently used in TPV systems, is around 0.6, however the emissivity of SiC range from 0.7 to 0.94 depending on author and measurement methodology [5]. Therefore, it is interesting to evaluate the average emissivity-dependant effect on the practical device performance.

Table 5 gives the computations of the open circuit voltage, short circuit current, fill factor and the conversion efficiency for all cases of the radiator effective emissivity with T_{Rad} = 1500k, T_{Cell} = 300k, $N_a = 5e^{20}$ cm^{-3}.

Table 5. Effect of the radiator emissivity on the photovoltaic parameters.

χ	**0.6**	**0.7**	**0.8**	**0.9**
V_{oc} (V)	0.400	0.404	0.407	0.410
I_{sc} (mA)	0.30	0.35	0.40	0.45
FF (%)	76.98	77.07	77.29	77.39
η (%)	26.73	26.83	27.71	27.74

While in figure 7, we have simulated the current-voltage characteristics as a function of χ.

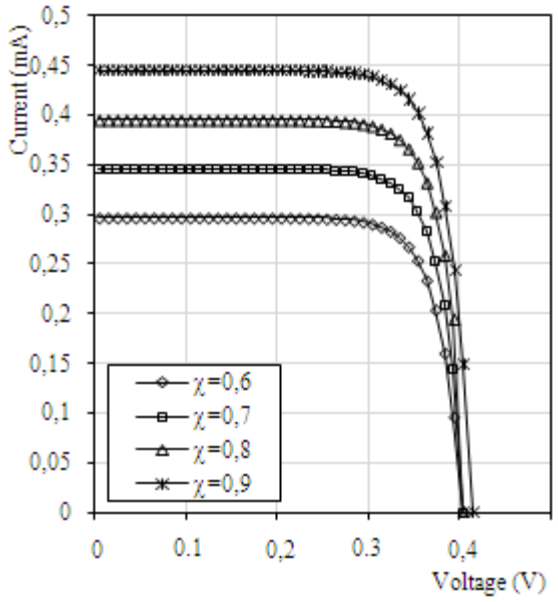

Fig. 7. Simulated current-voltage characteristics for different values of the effective emissivity.

It is seen, from the table and the figure above, that the efficiency improves from 26.73% for χ = 0.6 to 27.74% for χ = 0.9. Both open circuit voltage and the fill factor show little increment with the evolution of χ, whereas, the remaining parameters displays important improvements. So in order to achieve high conversion efficiency, it is important that the radiator has a high emissivity.

3.4. Effect of the radiator temperature

We simulated the current-voltage characteristic under four types of blackbody illumination spectrums with T_{Cell} = 300k, $N_a = 5e^{20}$ cm^{-3}, χ = 0.78, and the results were shown in figure 8. **Table 6** shows that the efficiency improves from 24.95% to 28.13% for 1300k and 1600k radiator's temperature respectively.

Table 6. Effect of the radiator temperature on the photovoltaic parameters.

T_{Rad} (k)	**1300**	**1400**	**1500**	**1600**
V_{oc} (V)	0.38	0.39	0.41	0.42
I_{sc} (mA)	0.13	0.24	0.39	0.60
FF (%)	76.12	76.97	77.26	77.69
η (%)	24.95	25.37	26.96	28.13

This improvement can be explained by taking into account that the increase in the radiator's temperature involves a significant increase in photocurrent for the reason that, as we saw in equation (8), the photocurrent is practically proportional to luminous flow, and owing to the fact that the open circuit voltage is also related to the short circuit current, it will undergo an increase and the conversion efficiency is always better in case of 1600k radiator's temperature.

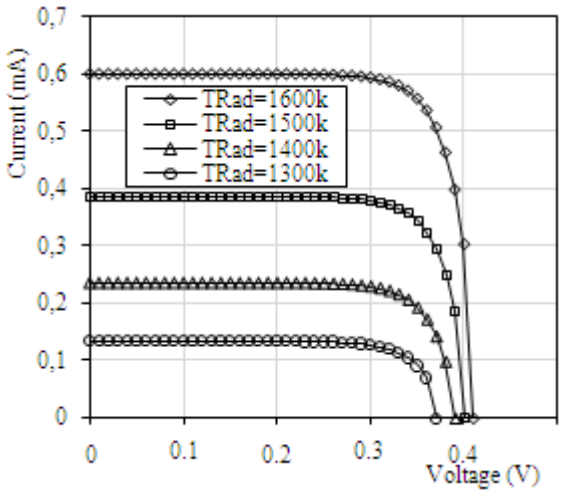

Fig. 8. Simulated current-voltage characteristics under four blackbody illumination spectrums.

These results are very similar to those obtained by V. Andreev et al. [24]. They simulated the conversion efficiency of GaSb TPV cells in the 1300k to 1500k temperature range and they obtained efficiencies of 24-26%. In addition, our results for 1600k radiator temperature are similar to those obtained by K. Qiu et al. [25]. They simulated the conversion efficiency of GaSb TPV cells in the 1073k to 1873k temperature range and they obtained a TPV efficiency of about 29% for1600k radiator temperature.

3.5. Effect of the cell temperature

As it is not realistic to operate a TPV cell at 300k, we have simulated the effect of elevated operating temperatures on the performance of the converter for $N_a = 5e^{20}$ cm^{-3} and χ = 0.78, under four types of blackbody illumination spectrums.

According to the results represented in **table 7** and the figure 9 below, it is seen that the increase of the cell's temperature causes a reduction in the bandgap width, therefore, the reverse saturation current will increase, causing a reduction in the open circuit voltage, and the mechanism of carrier's production becomes increasingly significant what implies a weak increase in the short circuit current.

It may be seen also that the fill factor undergoes a reduction with the increase of the cell's temperature following the increase in the dark saturation current, and owing to the fact that the reduction in the open circuit voltage is more significant with respect to the increase of the short circuit current, the conversion efficiency will also decrease.

Table 7. Effect of the cell temperature on the photovoltaic parameters.

T_{Rad} (k)	**1500**		
T_{Cell} (k)	**300**	**340**	**380**
Eg (ev)	0.72	0.70	0.68
I_0 (A)	$5.73e^{-11}$	$4.19e^{-09}$	$1.31e^{-07}$
V_{oc} (V)	0.41	0.34	0.27
I_{sc} (mA)	0.40	0.43	0.47
FF (%)	77.26	72.04	65.28
η (%)	26.96	23.32	18.21

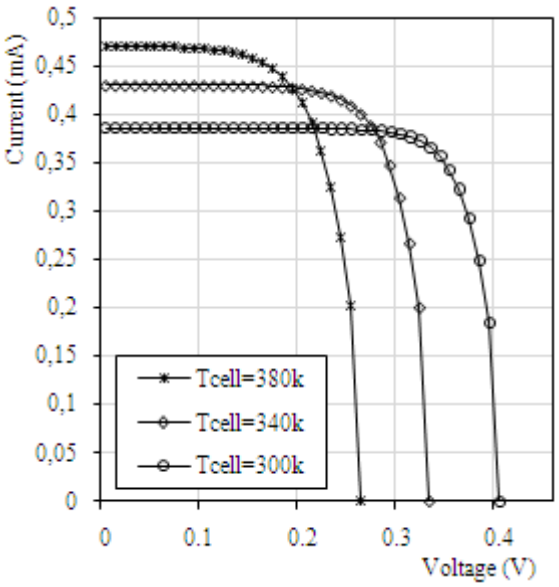

Fig. 9. Simulated current-voltage characteristics for different cell temperatures for T_{Rad} = 1500k.

4. Conclusion

In this study, we have improved a comprehensive model to predict the performance of a GaSb TPV converter heated by radio-isotopic source using a simulation program designed for this reason. Our results indicate that in order to achieve higher conversion efficiency, it is important to keep the base region doping as high as possible. Moreover, a cell thickness of about 60µm with low front recombination velocity is privileged to not contribute significantly in recombination.

It was found also that the conversion efficiency depends not only on the quality of the PV cell itself, but also on other external conditions as the specter quality, which depends strongly of the radiator emissivity and temperature. Our study proves that the spectrums of radiators operating at temperatures greater than 1500k, for an emissivity value of 0.78, contain significant proportion of incident radiations with energies sufficient to generate charge carriers in the PV cell and efficiencies exceeding 28% have been achieved by considering the cell's reflectance to the radiations with energy below the cell's bandgap.

The obtained results are found to be in good agreement with the available data.

In addition, we have analyzed the effect of elevated cell operating temperature on the conversion efficiency and we found that the increase of the cell temperature results a degradation of their performances.

References

[1] A. Luque and S. Hegedus, *Handbook of photovoltaic science and engineering*, John Wiley & Sons, England, 2003.

[2] V.M. Andreev, A.S. Vlasov, V.P. Khvostikov, O.A. Khvostikova, P.Y. Gazaryan, S.V. Sorokina, N.A. Sadchikov, "Solar thermophotovoltaic convertors based on tungsten emitters", *J. Sol. Energy Eng. – Trans. ASME 129*, pp. 298-303, 2007.

[3] A. Licciulli, D. Diso, G. Torsello, S. Tundo, A. Maffezzoli, M. Lomascolo, M. Mazzer, "The challenge of high-performance selective emitters for thermophotovoltaic applications", *Semiconductor Science and Technology*. Vol. 18, pp. 174-183, 2003.

[4] Donald L. Chubb, *Fundamentals of thermophotovoltaic energy conversion*, First Edition, Elsevier, 2007.

[5] T. Bauer, *Thermophotovoltaics Basic principles and critical aspects of system design*, Springer, 2011.

[6] W. M. Yang, S. K. Chou, C. Shu, Z. W. Li, H. Xue, "Research on micro-thermophotovoltaic power generators", *Solar Energy Materials & Solar Cells*, Vol. 80, pp. 95-104, 2003.

[7] [7] S. Malvadkar and E. Parsons, "Analysis of Potential Power Sources for Inspection Robots in Natural Gas Transmission Pipelines", Topical Report DE-FC26-01NT41155, *National Energy Technology Laboratory*, May 7, 2007.

[8] A. Schock, M. Mulcunda, C. Or, V. Kumar, and G. Summers, "Design, Analysis, and Optimization of a Radioisotope Thermo-photovoltaic (RTPV) Generator, and its Applicability to an Illustrative Space Mission", *Acta Astronautica*, Vol. 37, pp. 21-57, 1995.

[9] A. Kovacs and P. Janhunen, "Thermo-photovoltaic spacecraft electricity generation", *Astrophys. Space Sci. Trans*., 6, pp. 19-26, 2010.

[10] V. L. Teofilo, P. Choong, J. Chang, Y. L. Tseng and S. Ermer, "Thermophotovoltaic Energy Conversion for Space", *The journal of physical chemistry*, C, Vol. 112, pp. 7841-7845, 2008.

[11] S. M. Sze and K. K. Ng, *Physics of Semiconductor Devices*, Third Edition, John Wiley, Interscience, 2006.

[12] Y. Wang, N.F.Chen, X.W.Zhang, T.M.Huang, Z.G.Yin, Y.S.Wang, H.Zhang, "Evaluation of thermal radiation dependent performance of GaSb thermophotovoltaic cell based on an analytical absorption coefficient model", *Solar Energy Materials & Solar Cells*, Vol. 94, pp. 1704-1710, 2010.

[13] X. Peng, X. Guo, B. Zhang , X. Li, X. Zhao, X. Dong, W. Zheng, G. Du, "Numerical analysis of the short-circuit current density in GaInAsSb thermophotovoltaic diodes", *Infrared Physics & Technology*, Vol. 52, pp. 152-157, 2009.

[14] L.G. Ferguson, L.M. Fraas, "Theoretical study of GaSb PV cell efficiency as a function of temperature", *Solar Energy Materials & Solar Cells*, Vol. 39, pp. 11-18, 1995.

[15] N.N.Lal and A.W.Blakers, "Sliver Cells in Thermo-photovoltaic Systems", *Solar Energy Materials & Solar Cells*, Vol. 93, Issue 2, pp. 167-175, Feb. 2009.

[16] D. Martin, C. Algora, "Temperature-dependent GaSb material parameters for reliable Thermo-photovoltaic cell modeling*", Semicond. Sci. Technol*, Vol. 19, pp. 1040-1052, 2004.

[17] O.V. Sulima, A.W. Bett, "Fabrication and simulation of GaSb thermophotovoltaic cells", *Solar Energy Materials & Solar Cells*, Vol. 66, pp. 533-540, 2001.

[18] D.M. Caughey, R.E. Thomas, "Carrier mobility in Silicon empirically related to doping and field", *Proc. IEEE 55*, pp. 2192-2193, 1967.

[19] E. Rosencher, B. Vinter, *Optoélectronique*, Thomson-CSF, Masson, 1998.

[20] A. Chandola, R. Pino and P. S. Dutta, "Below bandgap optical absorption in tellurium-doped GaSb", *Semiconductor Science and Technology*, Vol. 20, pp. 886-893, 2005.

[21] L. L. Li, W. Xu, Z. Zeng, A. R. Wright, C. Zhang, J. Zhang, Y. L. Shi, "Mid-infrared absorption by short-period InAs/GaSb type II superlattices", *Microelectronics Journal*, Vol. 40, pp. 815-817, 2009.

[22] Ioffe Physico-Technical Institute: http://www.ioffe.rssi.ru/SVA/NSM/Semicond/GaSb/bandstr.html

[23] A. Ali, H. S. Madan, A. P. Kirk, D. A. Zhao, D. A. Mourey, M. K. Hudait, R. M. Wallace, T. N. Jackson, B. R. Bennett, J. B. Boos, and S. Datta, "Fermi level unpinning of GaSb (100) using plasma enhanced atomic layer deposition of Al_2O_3", *Applied Physics Letters*, Vol. 97, Issue 14, pp. 143502-143502-3 , 2010.

[24] V. Andreev, V. Khvostikov, and A. Vlasov, "Solar Thermophotovoltaics", *Springer Series in Optical Sciences*, Vol. 130/2007, pp.175-197, 2007.

[25] K. Qiu, A. C. S. Hayden, M. G. Mauk, O. V. Sulima, "Generation of electricity using InGaAsSb and GaSb TPV cells in combustion-driven radiant sources", *Solar Energy Materials & Solar Cells*, Vol. 90, pp. 68-81, 2006.»